INTERNATIONAL JOURNAL OF PROGRESSIVE RESEARCH IN ENGINEERING MANAGEMENT AND SCIENCE (IJPREMS)

www.ijprems.com
editor@ijprems.com

Vol. 04, Issue 07, July 2024, pp: 953-961

e-ISSN : 2583-1062

Impact Factor: 5.725

COMBINED EFFECTS OF SORET-DUFOUR, WITH HIGHER ORDER CHEMICAL REACTION IN MHD CASSON FLUID FLOW WITH VISCOUS DISSIPASSION THROUGH VERTICAL PLATE WITH HEAT SOURCE /SINK

A. K. Shukla[1], Santosh Kumar Chauhan[2], Vijayshree Yadav[3]

[1,2]Department of Mathematics, RSKD PG College Jaunpur-222001, India.

[3]Department of Applied science and Humanity, Dr. Ambedkar Institute of Technology for Divyangjan, Awadhpuri, Kanpur, India.

ABSTRACT

In this paper, we intend to develop the effects of Soret-Dufour, with Higher Order Chemical reaction in MHD Casson fluid flow with viscous dissipassion through vertical Plate with heat Source /Sink. A set of suitable local similarity transformations are used to non-dimensionalize the governing equations of the present problem. The system of partial differential equations are solved numerically by Crank-Nicolson finite difference Method. The effect of the involved parameters on velocity, Temperature, Concentration, Skin friction coefficient, Nusselt number and Sherwood number has been studied and numerical results are presented graphically and in tabular form.

Keywords: Magnetohydrodynamics, Soret and Dufour effect, Casson fluid, chemical reaction, Crank-Nicolson implicitfinitedifferencemethod

1. INTRODUCTION

Non-Newtonian fluids are significant in many engineering fields, particularly in the extraction of crude oil from petroleum-based products, such as polymer processing and the cleanup of nuclear reactor debris. Other industries include those that make paper, food, and clothing. medicines, blood flow, and plasma flow. Non-Newtonian fluids are always more suitable. unlike Newtonian. To understand the properties of non-Newtonian fluids and their uses, it's important to research their conductivity. The Casson fluid model is one kind of non-Newtonian fluid model proposed by Casson [1].

Raptis A et al. [2] analyse Effect of thermal radiation on magnetohydrodynamic flow. The radiation influence on MHD Casson fluid flow across an inclined non-linear surface with chemical reactions in a Forchheimer porous medium has been examined by Bejawada S. G. and Reddy Y. D. [3].

M. R. Eid et al. [4] have analysed a numerical study for Carreau nanofluid flow over a convectively heated nonlinear stretching surface with chemically reactive species. MHD casson fluid flow over a permeable stretching sheet with heat and mass transfer [5] was investigated by K. K. Asogwa and A. A. Ibe. Pandya N. and Shukla A. K. examined the effects of Soret, Dufour, Hall, and radiation on an unsteady MHD flow across an inclined plate with viscous dissipation, chemical reaction, and heat absorption and generation [6].

The effect of an aligned magnetic field and slanted outer velocity on casson fluid flow over a stretching sheet with a heat source has been examined by Renu Devi et al. [7]. The impact of Soret and Dufour on MHD Casson fluid flow past a stretching surface under convective-diffusive conditions has been studied by K Kumar Anantha et. al. [8]. The Casson fluid flow over a vertical porous surface with chemical reaction in the presence of a magnetic field [9].was studied by Emmanuel Maurice Arthur et al.

The numerical treatment of MHD flow of casson nanofluid via a convectively heated non-linear extending surface with viscous dissipation and suction/injection effects has been discovered by H. Alotaibi et al. [11]. K. Suneetha et al. [12] conducted a study on the free convective heat and mass transfer flow through a highly porous material with radiation, chemical reactions, and Soret effects. M. Mondal et al. [13] have provided a numerical investigation with stability convergence analysis of chemically hydromagnetic Casson fluid flow in the context of Brownian motion and thermophoresis.

The effects of outer velocity on the flow, heat transfer, and mass transfer of Casson nanofluid over a non-linear stretching sheet were examined by Vinita Makkar and Vikas Poply [14]. Studying the combined impacts of Soret-Dufour and a Higher Order Chemical Reaction in an MHD Casson fluid flow with viscous dissipation across a vertical plate with a heat source or sink is the goal of this work.

The CrankNicolson implicit finite difference method has been used to solve partial differential equations in non-dimensional form. Graphs are used to discuss the velocity, temperature, and concentration results that were obtained.

INTERNATIONAL JOURNAL OF PROGRESSIVE RESEARCH IN ENGINEERING MANAGEMENT AND SCIENCE (IJPREMS)

www.ijprems.com
editor@ijprems.com

Vol. 04, Issue 07, July 2024, pp: 953-961

e-ISSN : 2583-1062

Impact Factor: 5.725

2. MATHEMATICAL ANALYSIS

We are considering the combined effects of Soret-Dufour with higher-order chemical reactions in MHD Casson fluid flow with viscous dissipation through a vertical plate with a heat source/sink.The initial concentration and temperature of the plate are C^*_w and T^*_w respectively. The plate is assumed to be oriented x^* and y^*. y^* being normal to the plate. The plate's impulsive velocity is U_0. The induced magnetic field is ignored because the transverse applied magnetic field and Reynolds number are both very small. Following the aforementioned criteria, the velocity, temperature, and concentration equations in a Casson nanofluid are written as

$$\frac{\partial v^*}{\partial y^*} = 0 \Rightarrow \mathrm{v}^* = -\mathrm{V}_0 \qquad (1)$$

$$\frac{\partial u^*}{\partial t^*} + v^* \frac{\partial u^*}{\partial y^*} = \mathrm{v}\left(1+\frac{1}{\beta}\right)\left(\frac{\partial u^*}{\partial y^{*2}}\right) + g\beta t(T^* - T^*_\infty) \qquad (2)$$

$$+ g\beta_c(C^* - C^*_\infty) - \frac{\sigma B_0^2 u^*}{\rho} - \frac{\nu u^*}{K^*}$$

$$\rho c_p\left(\frac{\partial T*}{\partial t*} + v*\frac{\partial u*}{\partial y*}\right) = k\frac{\partial^2 T*}{\partial y*^2} - \frac{\partial q_r}{\partial y*}$$

$$+\rho\frac{D_m K_T}{c_s}\frac{\partial^2 C^*}{\partial y^{*2}} - Q_0\,(T^* - T^*_\infty) + \mu(\frac{\partial u*}{\partial y*})^2 \qquad (3)$$

$$\frac{\partial C^*}{\partial t^*} + v^*\frac{\partial^2 C^*}{\partial y^*} = D_m\frac{\partial^2 C^*}{\partial C^{*2}} + \frac{D_m K_T}{T_m}\frac{\partial^2 T^*}{\partial y^{*2}} - k_r(C^* - C^*_\infty)^n \qquad (4)$$

Where

$k_r(C^* - C^*_\infty)^n$	Terms in mass equation for higher order chemical reaction
n	Order of chemical reaction
k^r	Chemical reaction constant
C^*	Concentration
T^*	Temperature
T^*_∞	Temperature of free stream
C^*_∞	Concentration of free stream
β	Casson parameter
β_c	Coefficient of volume expansion for mass transfer
β_t	Volumetric coefficient of thermal expansion
T_m	Mean fluid temperature
q_r	Radiative heat along y ∗- axis
q_0	Coefficient of heat source/sink
v	Kinematic viscosity
K^*	Coefficient of permeability of porous medium
D_m	Molecular diffusivity
k	Thermal conductivity of fluid
c_p	Specific heat at constant pressure
μ	Viscosity
ρ	Fluid density
σ	Electrical conductivity
g	Acceleration due to gravity
K_T	Thermal diffusion ratio

intial and boundary conditions are:

INTERNATIONAL JOURNAL OF PROGRESSIVE RESEARCH IN ENGINEERING MANAGEMENT AND SCIENCE (IJPREMS)

e-ISSN : 2583-1062

www.ijprems.com
editor@ijprems.com

Vol. 04, Issue 07, July 2024, pp: 953-961

Impact Factor: 5.725

$u^* = 0\ T^* = T_\infty^*\ C^* = C_\infty^*\ for\ t^* \le 0\ and\ \forall\ y$

$u^* = U_0\ v^* = -V_0\ T^* = T_\infty^* + (T_w^* - T_\infty^*)e^{-Bt*}$ (5)

$C^* = C_\infty^* + (C_w^* - C_\infty^*)e^{-Bt*}, for\ t^* > 0\ and\ y^* = 0$

$u^* = 0\ T^* \to T_\infty^*\ C^* \to C_\infty^*\ for\ y^* \to \infty$

where the term T_w^* and C_w^* represent temperature and concentration respectively of plate and B is equivalent to $\frac{v_0^2}{v}$. The Radiative Heat flux termed by Roseland is approximately given by

$$q_r = -\frac{4\sigma_{st}}{3a_m}\frac{\partial T^{*4}}{\partial y^*} \quad (6)$$

where σst is Stefan Boltzmann constant and am is the mean absorption coefficient. In equation (6), term T_4^* can be expressed linearly, using Taylor's series about T_∞^* and neglect higher-order term because temperature difference within a flow is very small, so

$$T^{*4} \cong 4T_\infty^{*3}\ T^* - 3T_\infty^{*4} \quad (7)$$

with the help of equations (6) and (7), we can write the equation (3) as

$$\rho c_p\left(\frac{\partial T^*}{\partial t^*} + v^*\frac{\partial T^*}{\partial y^*}\right) = k\frac{\partial^2 T^*}{\partial y^{*2}} + \frac{16\sigma_{st}T_\infty^*}{3_{am}}\frac{\partial^2 T^*}{\partial y^*} + \frac{\rho D_m K_T}{c_s}\frac{\partial^2 T^*}{\partial y^{*2}} - Q_0(T^* - T_\infty^*) + \mu(\frac{\partial u^*}{\partial y^*}) \quad (8)$$

Let us introduce the following dimensionless quantities

$$Du = \frac{D_m K_T(C_w^* - C_\infty^*)}{c_s c_p \nu(T_w^* - T_\infty^*)}\quad Sr = \frac{D_m K_T(T_w^* - T_\infty^*)}{T_m \nu(C_w^* - C_\infty^*)}\quad u = \frac{u^*}{U_0}\quad t = \frac{t^* V_0^2}{v}$$

$$Gr = \frac{\nu g\beta_t(T_w^* - T_\infty^*)}{U_0\ V_0^2}\quad Gm = \frac{\nu g\beta_c(C_w^* - C_\infty^*)}{U_0\ V_0^2}\quad \theta = \frac{T^* - T_\infty^*}{T_w^* - T_\infty^*}$$

$$C = \frac{C^* - C_\infty^*}{C_w^* - C_\infty^*}\quad K = \frac{V_0^2 K^*}{v^2}\quad Pr = \frac{\mu c_p}{k}\quad M = \frac{\sigma B_0^2 \nu}{\rho V_0^2}$$

$$R = \frac{4\sigma_{st}T_\infty^{*3}}{a_m k}\quad Sc = \frac{\nu}{D_m}\quad y = \frac{y^* V_0}{\nu}\quad K_r = \frac{k_r \nu}{V_0^2}\quad Q = \frac{Q_0 \nu}{\rho c_p V_0^2}\quad Ec = \frac{U_0^2}{cp(T_w^* - T_\infty^*)} \quad (9)$$

To use non dimensional terms, introduced in equation (9), we get non-dimensional form of governing partial differential equations (2), (8) and (4) respectively:

$$\frac{\partial u}{\partial t} - \frac{\partial u}{\partial y} = \left(1 + \frac{1}{\beta}\right)\frac{\partial^2 u}{\partial y^2} + Gr\theta + GmC - \left(M + \frac{1}{K}\right)u \quad (10)$$

$$\frac{\partial \theta}{\partial t} - \frac{\partial \theta}{\partial y} = \frac{1}{Pr}(1 + \frac{4R}{3})\frac{\partial^2 \theta}{\partial y^2} + Du\frac{\partial 2C}{\partial y2} - Q\theta + Ec(\frac{\partial u}{\partial y})^2 \quad (11)$$

$$\frac{\partial C}{\partial t} - \frac{\partial C}{\partial y} = \frac{1}{Sc}\frac{\partial^2 C}{\partial y^2} + Sr\frac{\partial 2\theta}{\partial y2} - KrC^n \quad (12)$$

with initial and boundary conditions

$u = 0, \theta = 0, C = 0$ for $t \le 0$ and $\forall y$

$u = 1, \theta = e^{-t}, C = e^{-t}$ for $t > 0$ and $y = 0$ (13)

$u = 0, \theta \to 0, C \to 0$ for $y \to \infty$

The degree of practical attention include the Skin friction coefficients Cf , local Nusselt Nu, and local Sherwood Sh numbers are known as follows:

$$Cf = -(1 + \frac{1}{\beta})(\frac{\partial u}{\partial y})_{y=0}$$

$$Nu = -(\frac{\partial \theta}{\partial y})_{y=0} \quad (14)$$

$$Sh = -(\frac{\partial C}{\partial y})_{y=0}$$

3. METHOD OF SOLUTION

The aforementioned nonlinear partial differential equation (10-12) linked to the initial and boundary conditions (13) is solved using the Crank-Nicolson implicit finite difference method. The Crank-Nicolson implicit finite difference technique is an unconditionally stable second-order method that is ($o\ (\Delta t^2)$) in time and has no space or time step limitations. Until y = 4, the calculation is run for Δy = 0.1, to Δt = 0.001, and the process is repeated. As we are employing the Crank-Nicolson implicit finite difference approach, the velocity equation (10), the energy equation (11), and the equation of conservation of species (12) are all written in their transient forms.

INTERNATIONAL JOURNAL OF PROGRESSIVE RESEARCH IN ENGINEERING MANAGEMENT AND SCIENCE (IJPREMS)

www.ijprems.com
editor@ijprems.com

Vol. 04, Issue 07, July 2024, pp: 953-961

e-ISSN : 2583-1062

Impact Factor: 5.725

$$\frac{u_{i,j+1}-u_{i,j}}{\Delta t}-\frac{u_{i+1,j}-u_{i,j}}{\Delta y}=\left(1+\frac{1}{\beta}\right)\frac{u_{i-1,j}-2u_{i,j}+u_{i+1,j}+u_{i-1,j+1}-2u_{i,j+1}+u_{i+1,j+1}}{2(\Delta y)^2}$$
$$+G_r\left(\frac{\theta_{i,j+1}+\theta_{i,j}}{2}\right)+G_m\left(\frac{C_{i,j+1}+C_{i,j}}{2}\right)-\left(M+\frac{1}{K}\right)\left(\frac{u_{i,j+1}+u_{i,j}}{2}\right) \quad (15)$$

$$\frac{\theta_{i,j+1}-\theta_{i,j}}{\Delta t}-\frac{\theta_{i+1,j}-\theta_{i,j}}{\Delta y}=\frac{1}{P_r}\left(1+\frac{4R}{3}\right)\left(\frac{\theta_{i-1,j}-2\theta_{i,j}+\theta_{i+1,j}+\theta_{i-1,j+1}-2\theta_{i,j+1}+\theta_{i+1,j+1}}{2(\Delta y)^2}\right)$$
$$+D_u\left(\frac{C_{i-1,j}-2C_{i,j}+C_{i+1,j}+C_{i-1,j+1}-2C_{i,j+1}+C_{i+1,j+1}}{2(\Delta y)^2}\right)-Q\left(\frac{\theta_{i,j+1}+\theta_{i,j}}{2}\right)+E_C\left(\frac{u_{i+1,j}-u_{i,j}}{\Delta y}\right)^2 \quad (16)$$

$$\frac{C_{i,j+1}-C_{i,j}}{\Delta t}-\frac{C_{i+1,j}-C_{i,j}}{\Delta y}=\frac{1}{S_C}\left(\frac{C_{i-1,j}-2C_{i,j}+C_{i+1,j}+C_{i-1,j+1}-2C_{i,j+1}+C_{i+1,j+1}}{2(\Delta y)^2}\right)$$
$$+S_r\left(\frac{\theta_{i-1,j}-2\theta_{i,j}+\theta_{i+1,j}+\theta_{i-1,j+1}-2\theta_{i,j+1}+\theta_{i+1,j+1}}{2(\Delta y)^2}\right)+K_r\left(\frac{C_{i,j+1}+C_{i,j}}{n}\right)^2 \quad (17)$$

and transient form of initial and boundary conditions are:

$$u_{i,0}=0,\quad \theta_{i,0}=0,\quad C_{i,0}=0 \quad \text{for all} \quad i=1,2,3,\ldots$$
$$u_{0,j}=1,\quad \theta_{0,j}=e^{-j\Delta t},\quad C_{0,j}=e^{-j\Delta t} \quad \text{for all} \quad j=1,2,3,\ldots \quad (18)$$
$$u_{n,j}=0,\theta_{n,j}\to 0,C_{n,j}\to 0$$

where y denotes the spatial direction and i the temporal direction. Defined as t, $\Delta y = y_{i+1}-y_i$, and $\Delta t = t_{j+1}-t_j$. The values at time t + Δt can be computed using the following method to determine the values of u, θ, and C at time t.Equations (15) to (17), which give a tridiagonal system of equations with boundary conditions in equation (18), are solved using the Thomos algorithm as detailed in Carnahan et al. [10] by replacing i = 1, 2, ..., N − 1, where N correspond to ∞.For all values of y at t + Δt, we find values of θ and C.The same method is used to solve equation (15) so that by substituting these values for θ and C, we can obtain a solution for u up to the desired time t.

4. RESULTS AND DISCUSSION

In order of analysis, numerically calculated consequences are shown, both graphically and numerically. In this analysis, the values of the parameters, Chemical reaction parameter Kr = 1.2, Dufour number Du = 0.2, heat source/sink parameter Q = 2, Soret number Sr = 1.5, Schmidt number Sc = 0.6, order of chemical reaction n = 2, radiation parameter R = 2.2, magnetic parameter M = 4.8, Casson β = 0.4, t = 0.2, Grashof number Gr = 4,solutal Grashof number Gm = 7, K = 1.5 and Prandtl number P r = 0.7 are kept constant in the whole calculation unless otherwise stated in the respective graphs and tables. The numerical results for various profiles, such as the velocity profile u along the x-axis, the temperature profile θ, and the concentration profile C, are shown. Figure 1 depicts the effect of the Dufour number on the concentration profile C, which decreases as the Dufour number increases. The concentration profile C in figure 2 decreases as the Eckert no Ec increases. In Figures 3, 6, and 7, increasing the chemical reaction parameter Kr, the radiation parameter R, and the Schmidt number Sc causes the concentration profile C to decrease; increasing the Prandtl number P r and the heat source/sink parameter Q causes the concentration profile C to increase and then decrease after some distance in figures 4, 5. The concentration profile C in figure 8 increases with increasing Soret no Sr. The temperature profile θ increases with increasing Dufour number Du, Eckert number Ec, and radiation parameter R in figures 9, 10, and 13, but decreases with increasing Prandtl number P r and heat source/sink parameter Q in figures 11 and 12. In the figures 15, 16, 21, and 26, the velocity profile increases as the Dufour number Du, Eckert number Ec, radiation parameter R, and Soret number Sr increase. The velocity profile decreases in figures 17, 18, 19, 20 and 22 on increasing chemical reaction parameter Kr, magnetic parameter M, Prandtl number P r, heat source/sink parameter Q, and Schmidt number Sc. The velocity profile increases as the cassion fluid parameter Bt increases, and then decreases (see figure 14. In figure 23, 25 and 24 the Concentration profile C, velocity Profile u and Temperature profile θ increases with time. Table 1 provides change of Skin friction coefficient Cf , Nusselt number Nu and Sherwood number Sh for the different values of parameters.

INTERNATIONAL JOURNAL OF PROGRESSIVE RESEARCH IN ENGINEERING MANAGEMENT AND SCIENCE (IJPREMS)

www.ijprems.com
editor@ijprems.com

Vol. 04, Issue 07, July 2024, pp: 953-961

e-ISSN : 2583-1062

Impact Factor: 5.725

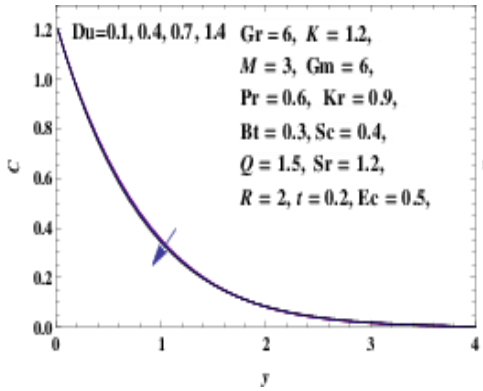

Figure 1: Concentration Profile (C) for Different Values of Du

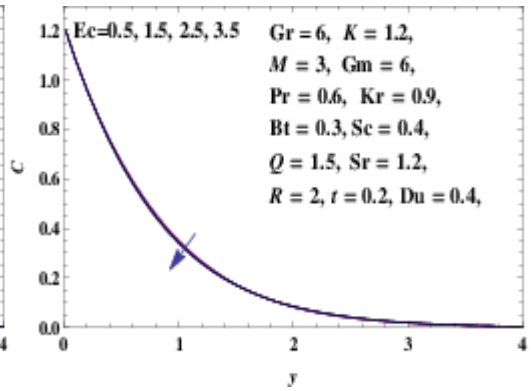

Figure 2: Concentration Profile (C) for Different Values of Ec

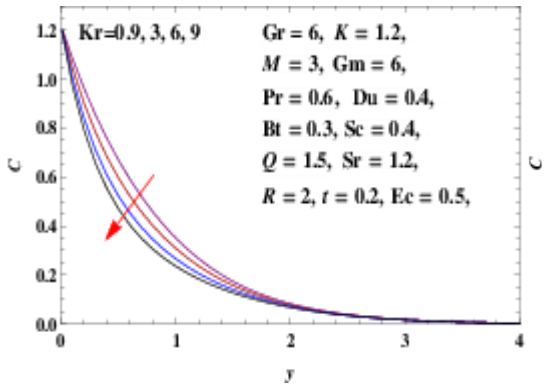

Figure 3: Concentration Profile (C) for Different Values of

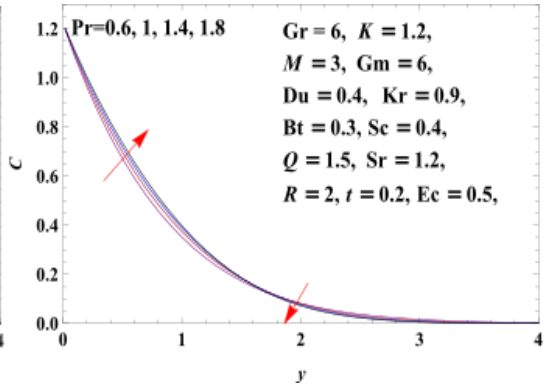

Figure 4: Concentration Profile (C) for Different Values of Pr

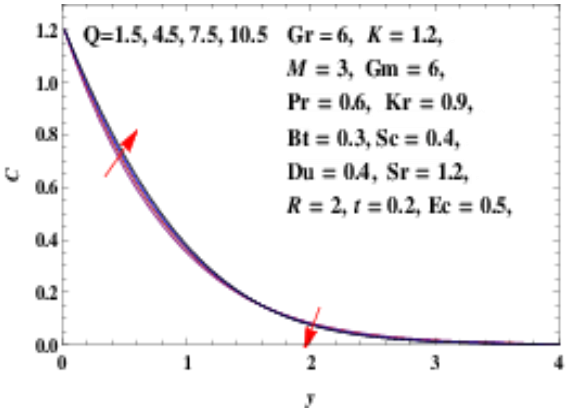

Figure 5: Concentration Profile (C) for Values of Q

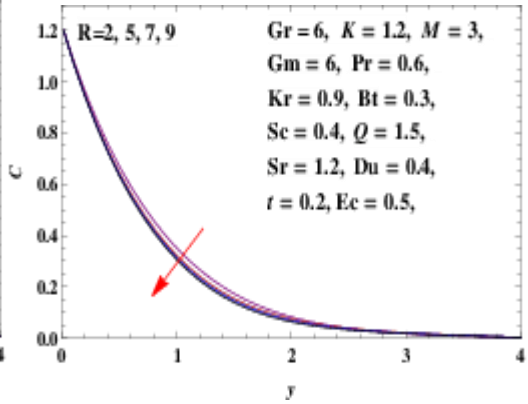

Figure 6: Concentration Profile (C) for Different Different Values of R

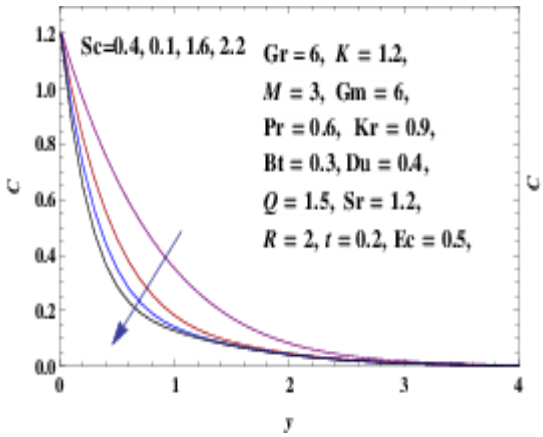

Figure 7: Concentration Profile (C) for Different Values of Sc

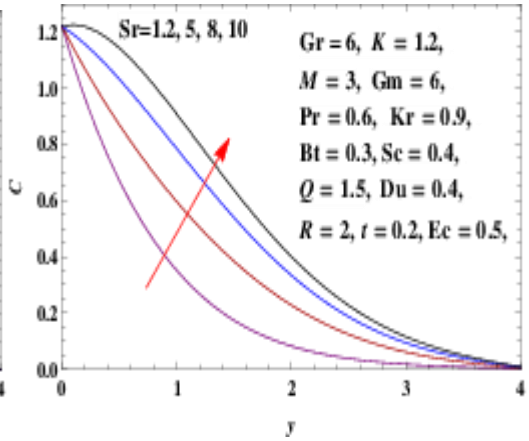

Figure 8: Concentration Profile (C) for Different Values of Sr

INTERNATIONAL JOURNAL OF PROGRESSIVE RESEARCH IN ENGINEERING MANAGEMENT AND SCIENCE (IJPREMS)

www.ijprems.com
editor@ijprems.com

Vol. 04, Issue 07, July 2024, pp: 953-961

e-ISSN : 2583-1062

Impact Factor: 5.725

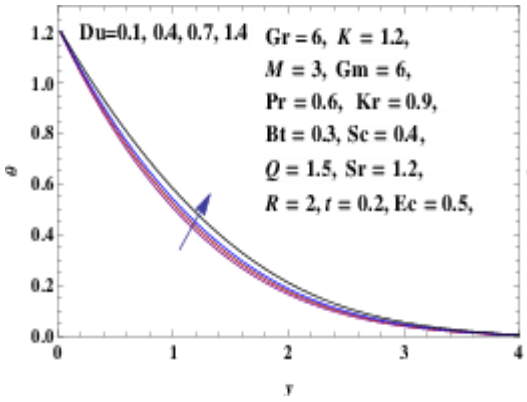

Figure 9: Temperature Profile (θ) for Values of Du

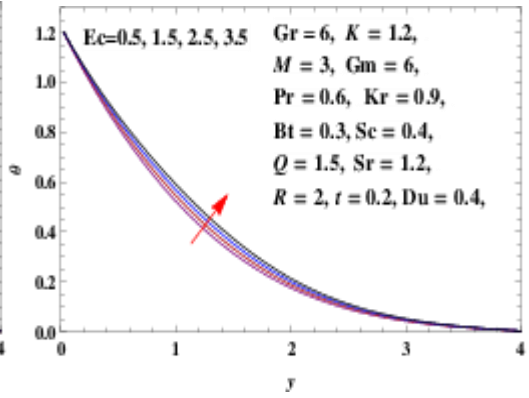

Figure 10: Temperature Profile (θ) for Different Different Values of Ec

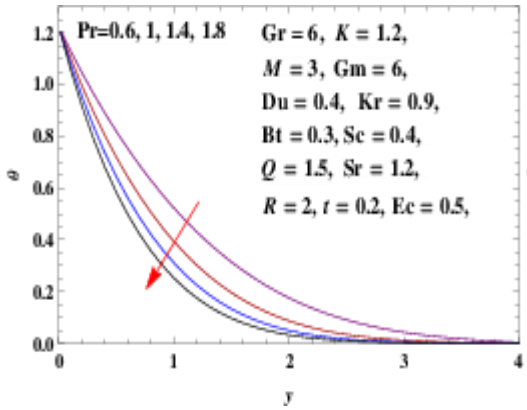

Figure 11: Temperature Profile (θ) for Different Values of Pr

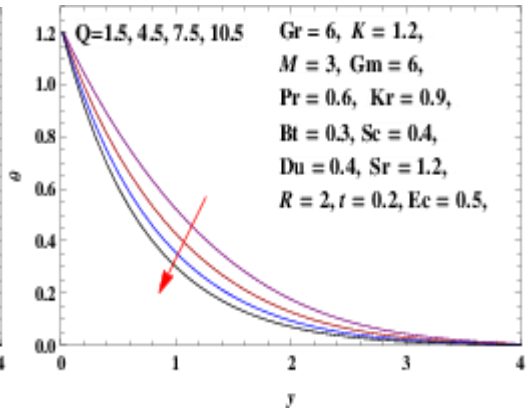

Figure 12: Temperature Profile (θ) for Different Values of Q

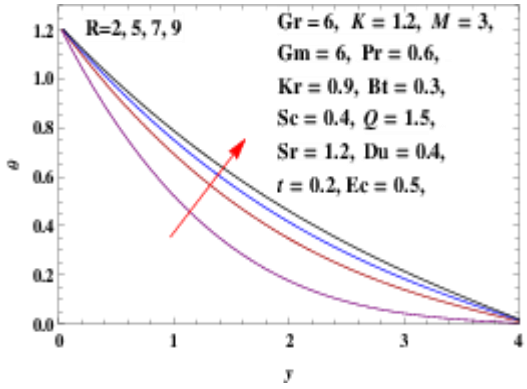

Figure 13: Temperature Profile (θ) for Different Values of R

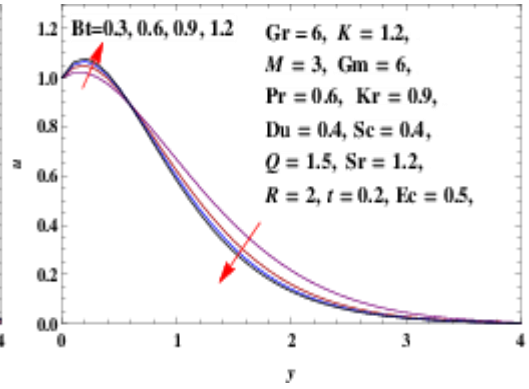

Figure 14: Velocity Profile (u) for Different Values of Bt

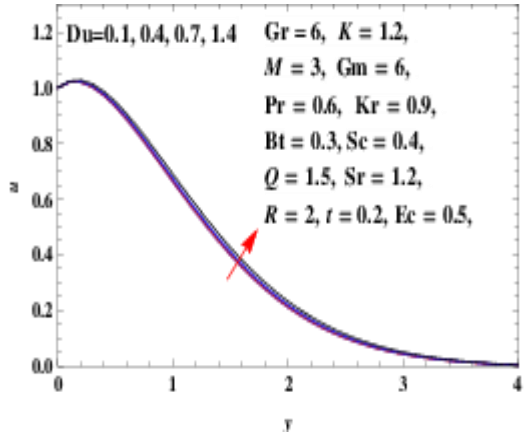

Figure 15: Velocity Profile (u) for Different Values of Du

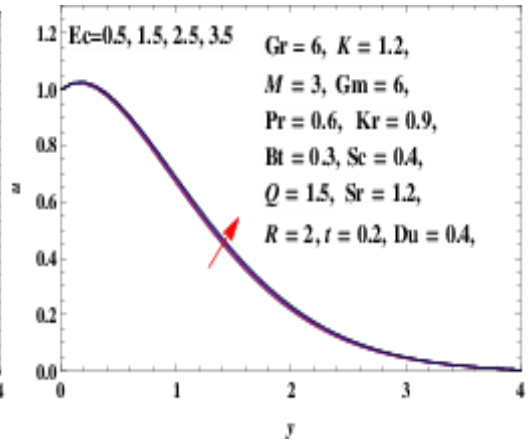

Figure 16: Velocity Profile (u) for Different Values of Ec

INTERNATIONAL JOURNAL OF PROGRESSIVE RESEARCH IN ENGINEERING MANAGEMENT AND SCIENCE (IJPREMS)

www.ijprems.com
editor@ijprems.com

Vol. 04, Issue 07, July 2024, pp: 953-961

e-ISSN : 2583-1062

Impact Factor: 5.725

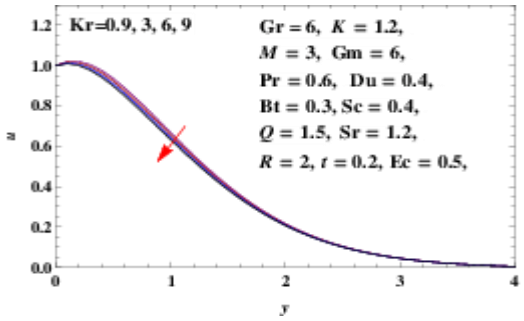

Figure 17: Velocity Profile (u) for Different Values of Kr

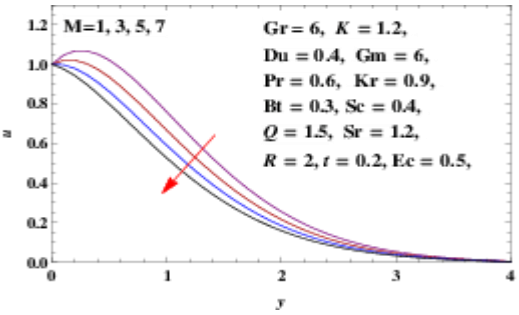

Figure 18: Velocity Profile (u) for Different Values of M

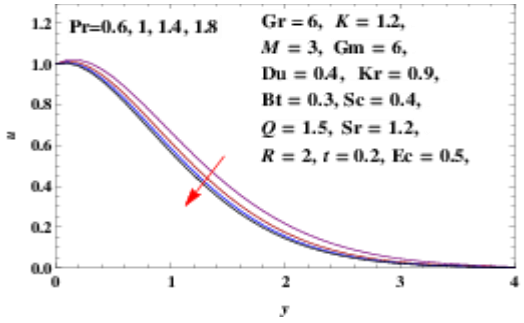

Figure 19: Velocity Profile (u) for Different Values of P r

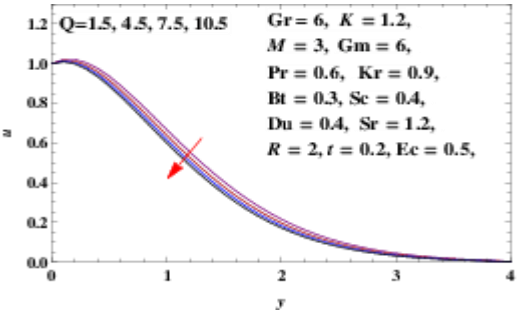

Figure 20: Velocity Profile (u) for Different Values of Q

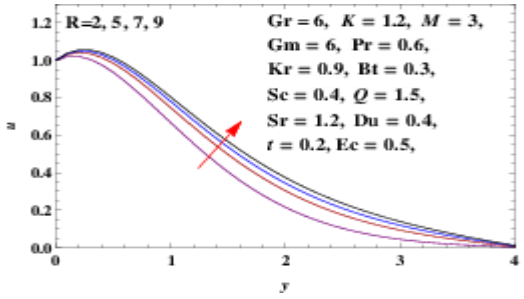

Figure 21: Velocity Profile (u) for Different Values of R

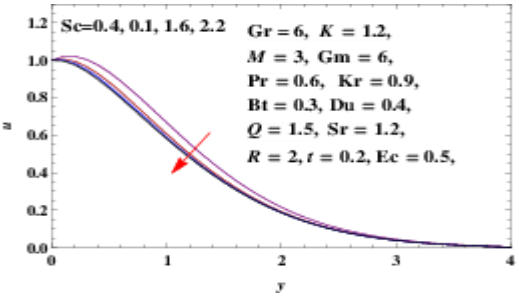

Figure 22: Velocity Profile (u) for Different Values of Sc

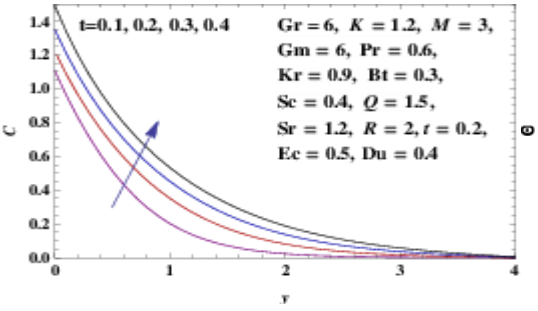

Figure 23: Concentration Profile (C) for Different Values of t

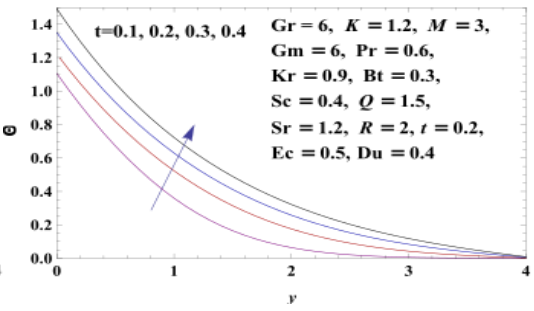

Figure 24: Temperature Profile (θ) for Different Values of t

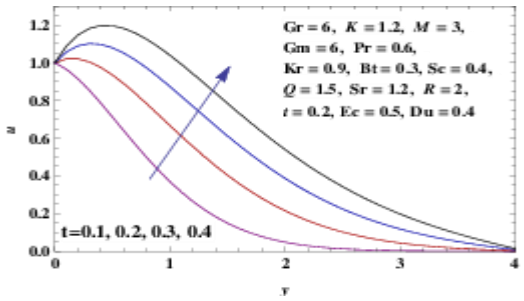

Figure 25: Velocity Profile (u) for Different Values of t

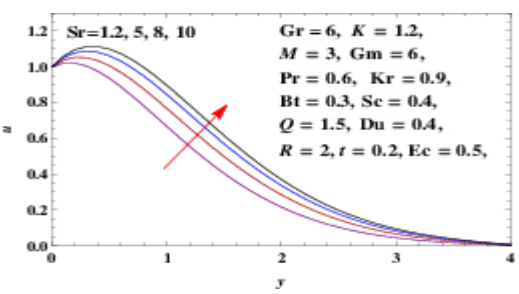

Figure 26: Velocity Profile (u) for Different Values of Sr

INTERNATIONAL JOURNAL OF PROGRESSIVE RESEARCH IN ENGINEERING MANAGEMENT AND SCIENCE (IJPREMS)

www.ijprems.com
editor@ijprems.com

Vol. 04, Issue 07, July 2024, pp: 953-961

e-ISSN : 2583-1062

Impact Factor: 5.725

Table1: Skin friction coefficients τ, Nu and Sh for different values of parameters

Bt	Du	Ec	Kr	M	Pr	Q	R	Sc	Sr	t	τ	Nu	Sh
0.3	0.4	0.5	0.9	3	0.6	1.5	2	0.4	1.2	0.2	−0.89905	0.907231	1.35949
0.6	0.4	0.5	0.9	3	0.6	1.5	2	0.4	1.2	0.2	−1.10911	0.903068	1.36075
0.9	0.4	0.5	0.9	3	0.6	1.5	2	0.4	1.2	0.2	−1.1454	0.900797	1.36144
1.2	0.4	0.5	0.9	3	0.6	1.5	2	0.4	1.2	0.2	−1.1513	0.899344	1.36189
0.3	0.1	0.5	0.9	3	0.6	1.5	2	0.4	1.2	0.2	−0.856126	0.948593	1.34577
0.3	0.4	0.5	0.9	3	0.6	1.5	2	0.4	1.2	0.2	−0.89905	0.907231	1.35949
0.3	0.7	0.5	0.9	3	0.6	1.5	2	0.4	1.2	0.2	−0.9425	0.864594	1.37372
0.3	1.4	0.5	0.9	3	0.6	1.5	2	0.4	1.2	0.2	−1.04602	0.75971	1.40909
0.3	0.4	0.5	0.9	3	0.6	1.5	2	0.4	1.2	0.2	−0.89905	0.907231	1.35949
0.3	0.4	1.5	0.9	3	0.6	1.5	2	0.4	1.2	0.2	−0.947613	0.872918	1.3698
0.3	0.4	2.5	0.9	3	0.6	1.5	2	0.4	1.2	0.2	−0.995902	0.839295	1.37986
0.3	0.4	3.5	0.9	3	0.6	1.5	2	0.4	1.2	0.2	−1.04392	0.80633	1.3897
0.3	0.4	0.5	0.9	3	0.6	1.5	2	0.4	1.2	0.2	−0.89905	0.907231	1.35949
0.3	0.4	0.5	3	3	0.6	1.5	2	0.4	1.2	0.2	−0.733051	0.885407	1.74071
0.3	0.4	0.5	6	3	0.6	1.5	2	0.4	1.2	0.2	−0.556237	0.861402	2.15116
0.3	0.4	0.5	9	3	0.6	1.5	2	0.4	1.2	0.2	−0.423015	0.842558	2.46781
0.3	0.4	0.5	0.9	1	0.6	1.5	2	0.4	1.2	0.2	−2.03313	0.907252	1.35919
0.3	0.4	0.5	0.9	3	0.6	1.5	2	0.4	1.2	0.2	−0.89905	0.907231	1.35949
0.3	0.4	0.5	0.9	5	0.6	1.5	2	0.4	1.2	0.2	0.0981792	0.906299	1.36008
0.3	0.4	0.5	0.9	7	0.6	1.5	2	0.4	1.2	0.2	0.984251	0.904842	1.36083
0.3	0.4	0.5	0.9	3	0.6	1.5	2	0.4	1.2	0.2	−0.89905	0.907231	1.35949
0.3	0.4	0.5	0.9	3	1	1.5	2	0.4	1.2	0.2	−0.578762	1.18265	1.27252
0.3	0.4	0.5	0.9	3	1.4	1.5	2	0.4	1.2	0.2	−0.373304	1.41444	1.19335
0.3	0.4	0.5	0.9	3	1.8	1.5	2	0.4	1.2	0.2	−0.224559	1.6218	1.11899
0.3	0.4	0.5	0.9	3	0.6	1.5	2	0.4	1.2	0.2	−0.89905	0.907231	1.35949
0.3	0.4	0.5	0.9	3	0.6	4.5	2	0.4	1.2	0.2	−0.695237	1.18223	1.27751
0.3	0.4	0.5	0.9	3	0.6	7.5	2	0.4	1.2	0.2	−0.530828	1.41473	1.20386
0.3	0.4	0.5	0.9	3	0.6	10.5	2	0.4	1.2	0.2	−0.395866	1.61585	1.13694
0.3	0.4	0.5	0.9	3	0.6	1.5	2	0.4	1.2	0.2	−0.89905	0.907231	1.35949
0.3	0.4	0.5	0.9	3	0.6	1.5	5	0.4	1.2	0.2	−1.35955	0.624893	1.43769
0.3	0.4	0.5	0.9	3	0.6	1.5	7	0.4	1.2	0.2	−1.53607	0.541119	1.45873
0.3	0.4	0.5	0.9	3	0.6	1.5	9	0.4	1.2	0.2	−1.66271	0.488362	1.47195
0.3	0.4	0.5	0.9	3	0.6	1.5	2	0.4	1.2	0.2	−0.89905	0.907231	1.35949
0.3	0.4	0.5	0.9	3	0.6	1.5	2	1	1.2	0.2	−0.299819	0.857443	2.1945
0.3	0.4	0.5	0.9	3	0.6	1.5	2	1.6	1.2	0.2	−0.0250622	0.818279	2.83285
0.3	0.4	0.5	0.9	3	0.6	1.5	2	2.2	1.2	0.2	0.145401	0.784065	3.38333
0.3	0.4	0.5	0.9	3	0.6	1.5	2	0.4	1.2	0.2	−0.89905	0.907231	1.35949
0.3	0.4	0.5	0.9	3	0.6	1.5	2	0.4	5	0.2	−1.61209	0.939566	0.785855
0.3	0.4	0.5	0.9	3	0.6	1.5	2	0.4	8	0.2	−2.18319	0.966904	0.29475
0.3	0.4	0.5	0.9	3	0.6	1.5	2	0.4	10	0.2	−2.56893	0.986259	−0.0552378

0.3	0.4	0.5	0.9	3	0.6	1.5	2	0.4	1.2	0.1	1.49586	0.965786	1.45286
0.3	0.4	0.5	0.9	3	0.6	1.5	2	0.4	1.2	0.2	−0.89905	0.907231	1.35949
0.3	0.4	0.5	0.9	3	0.6	1.5	2	0.4	1.2	0.3	−2.4789	0.940984	1.42565
0.3	0.4	0.5	0.9	3	0.6	1.5	2	0.4	1.2	0.4	−3.80777	1.00593	1.55603

5. CONCLUSION

In this paper, we have studied the combined effects of Soret-Dufour with higher-order chemical reactions in MHDCasson fluid flow with viscous dissipation through a vertical plate with a heat source /sink. We can draw the following conclusions from our investigation of this problem:

1. When the casson fluid parameter is increased, the skin friction coefficient and Nusselt number decrease, while the Sherwood number increases.
2. The skin friction coefficient decreases when the Dufour number increases.
3. The velocity decreases as the heat source/sink parameter is increased.
4. The velocity decreases with an increase in the chemical reaction parameter.

6. REFERENCES

[1] T. Mohana Priya, Dr. M. Punithavalli& Dr. R. Rajesh Kanna, Machine Learning Algorithm for Development of Enhanced Support Vector Machine Technique to Predict Stress, Global Journal of Computer Science and Technology: C Software & Data Engineering, Volume 20, Issue 2, No. 2020, pp 12-20

[2] Ganesh Kumar and P.Vasanth Sena, “Novel Artificial Neural Networks and Logistic Approach for Detecting Credit Card Deceit,” International Journal of Computer Science and Network Security, Vol. 15, issue 9, Sep. 2015, pp. 222-234

[3] Gyusoo Kim and Seulgi Lee, “2014 Payment Research”, Bank of Korea, Vol. 2015, No. 1, Jan. 2015.

[4] Chengwei Liu, Yixiang Chan, Syed Hasnain Alam Kazmi, Hao Fu, “Financial Fraud Detection Fluid: Based on Random Forest,” International Journal of Economics and Finance, Vol. 7, Issue. 7, pp. 178-188, 2015.

[5] Hitesh D. Bambhava, Prof. Jayeshkumar Pitroda, Prof. Jaydev J. Bhavsar (2013), “A Comparative Study on Bamboo Scaffolding And Metal Scaffolding in Construction Industry Using Statistical Methods”, International Journal of Engineering Trends and Technology (IJETT) – Volume 4, Issue 6, June 2013, Pg.2330-2337.